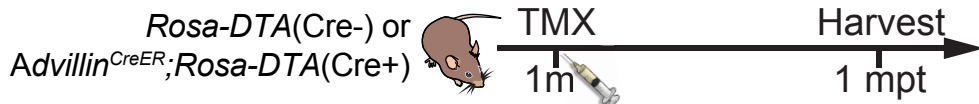
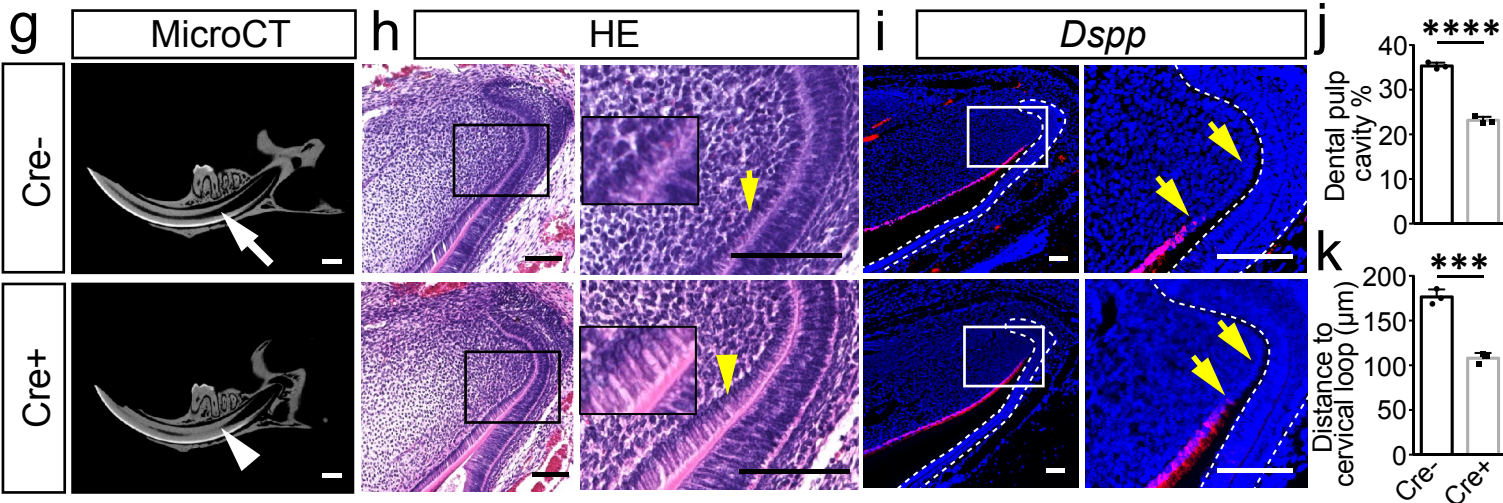
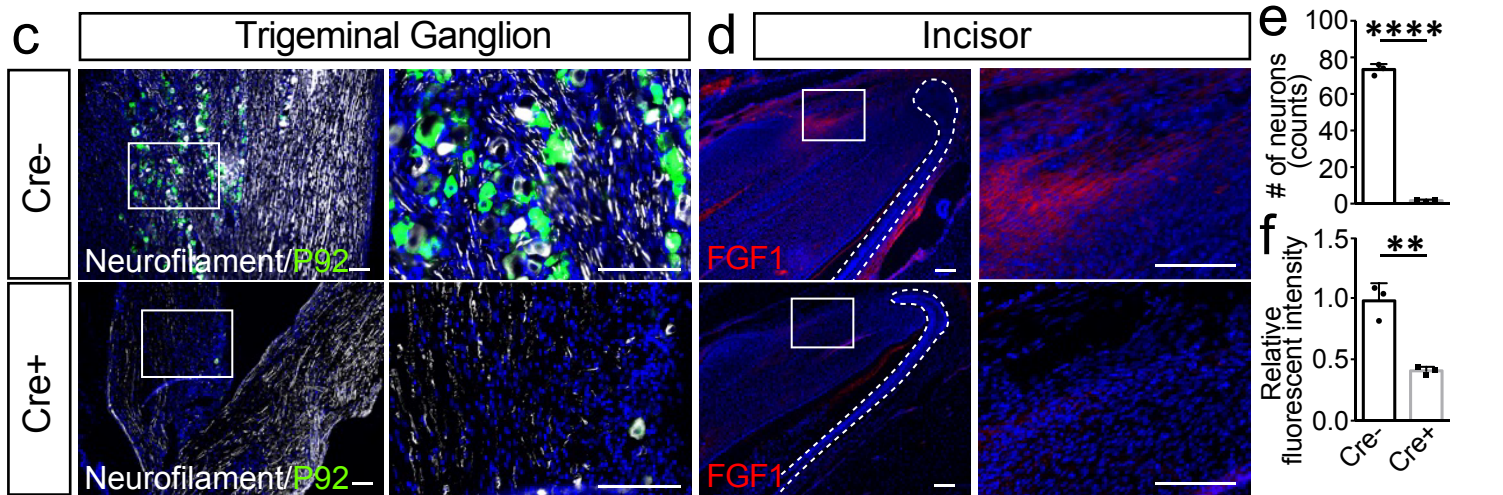
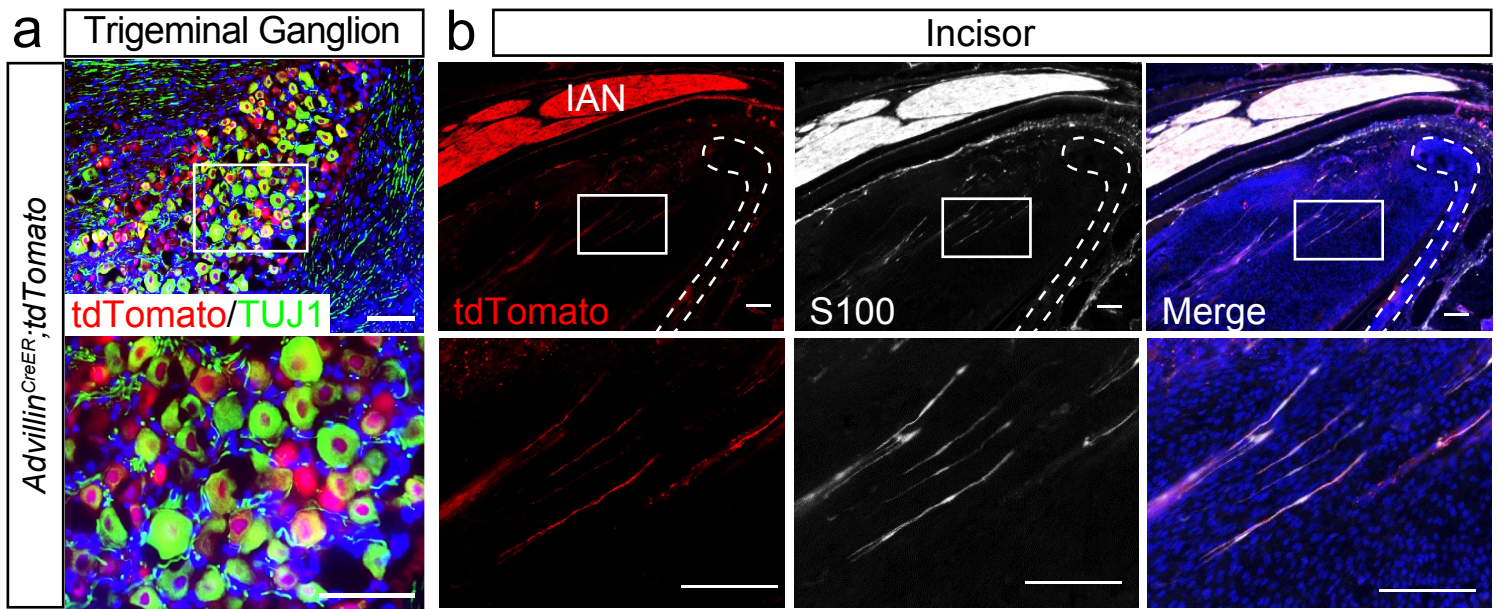


Sensory nerve niche regulates mesenchymal stem cell homeostasis via
FGF/mTOR/autophagy axis

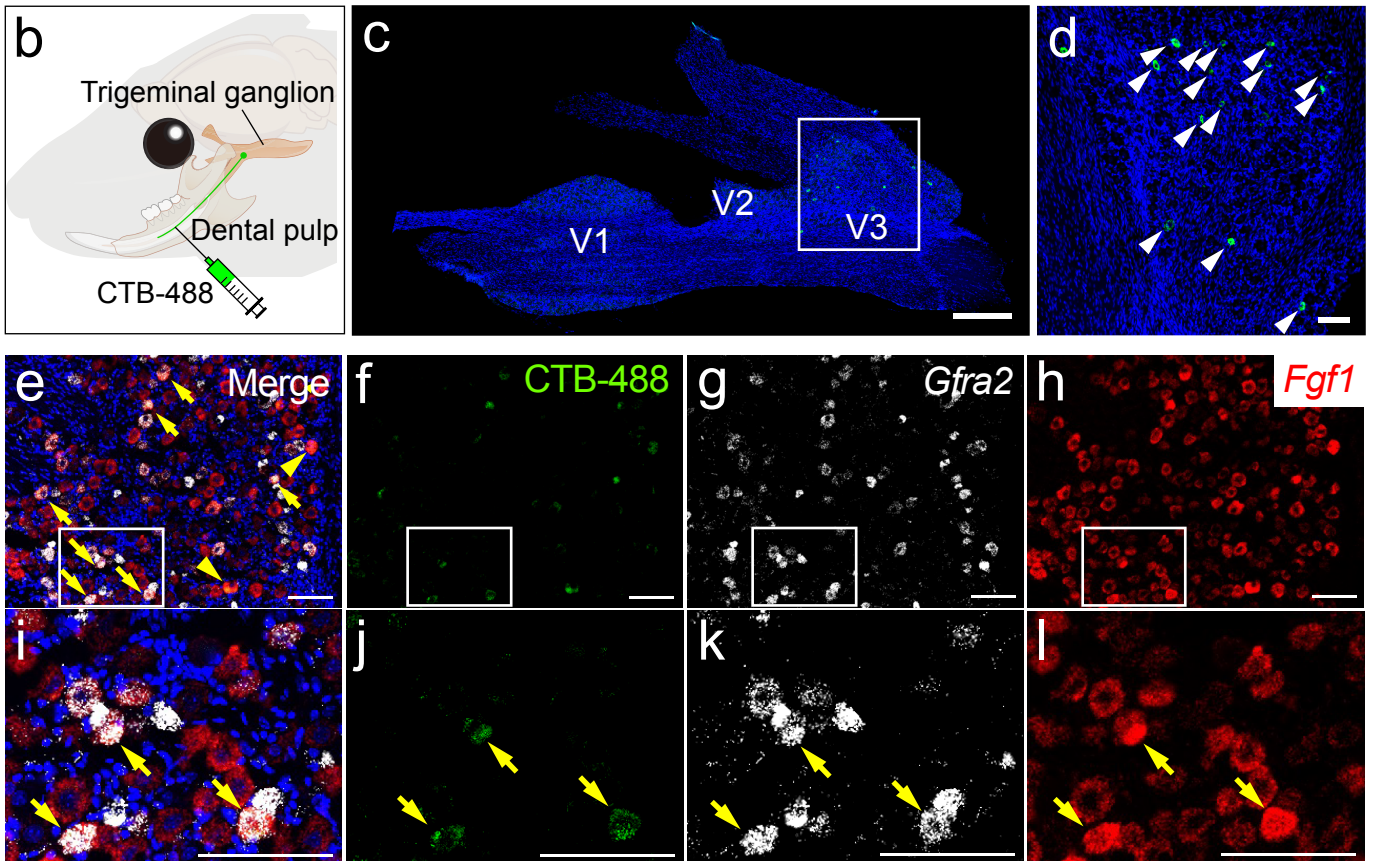
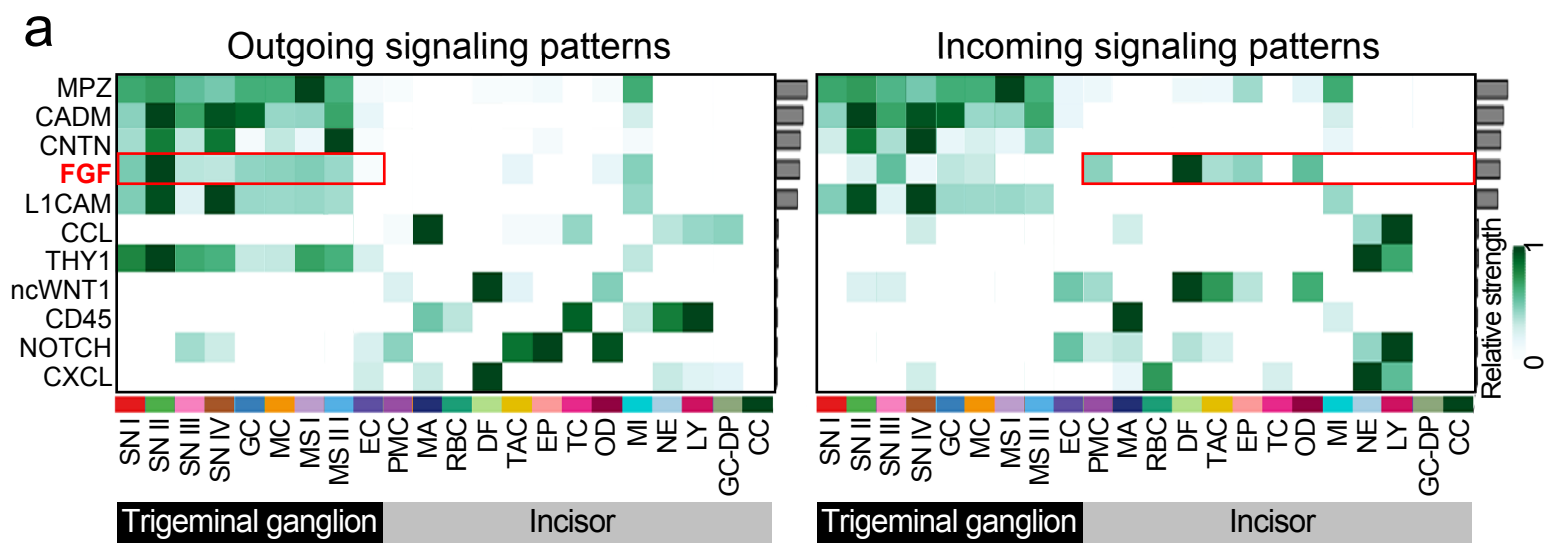
This document includes:

Supplementary Fig.1 to Supplementary Fig. 8



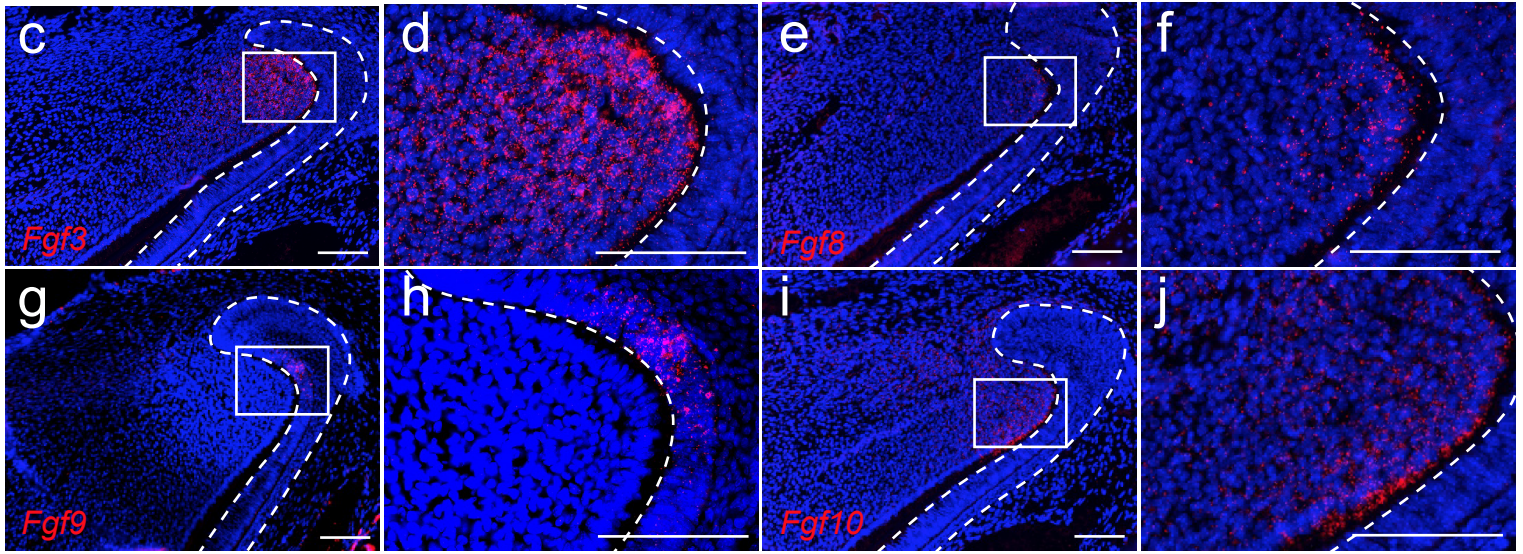
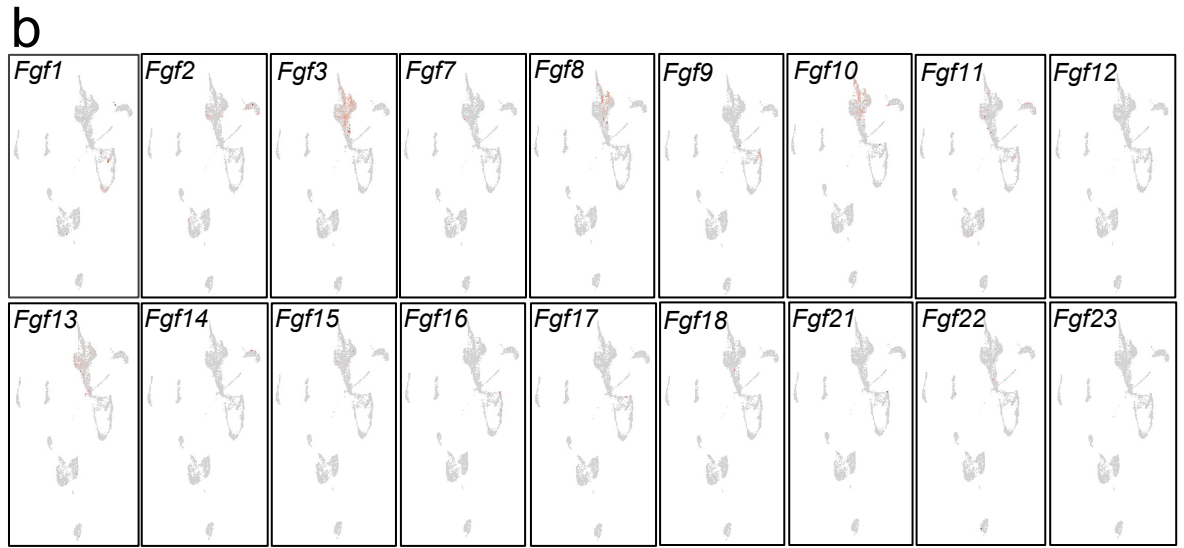
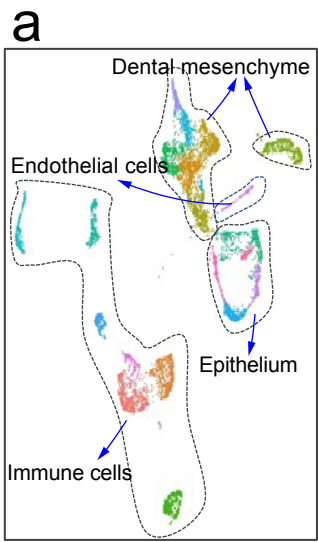
Supplementary Fig. 1: Deletion of sensory nerve leads to abnormal dentin formation.

a Colocalization of tdTomato and nerve marker TUJ1 in the trigeminal ganglion of *Advillin^{CreER};tdTomato* mice 7 days after induction. **b** *Advillin* targeted inferior alveolar nerve (IAN) and nerve fibers in the incisor of *Advillin^{CreER};tdTomato* mice. Expression of tdTomato in IAN and nerves in the incisor, and colocalized with nerve marker S100. **c** Sensory neurons stained with P92 in the trigeminal ganglion of control and *Advillin^{CreER};Rosa-DTA* mice one month after tamoxifen induction. **d** Expression of FGF1 decreased in the incisor one month after sensory nerve deletion. **e** Quantification of neuron numbers in trigeminal ganglion in control and *Advillin^{CreER};Rosa-DTA* mice. $P < 0.0001$. **f** Quantification of relative fluorescent intensity of FGF1 in control and mutant mice. $P = 0.0026$. **g** CT scanning of control and *Advillin^{CreER};Rosa-DTA* mice one month after tamoxifen induction. White arrow points to dental pulp cavity; white arrowhead points to narrowed pulp cavity. **h** Histological analysis of control and *Advillin^{CreER};Rosa-DTA* mice one month after induction. Yellow arrow points to pre-odontoblast; yellow arrowhead points to abnormal pre-odontoblast. **i** *Dspp* expression in control and mutant mice. Yellow arrow points to the distance between the bending point of the cervical loop and the initiation of odontoblast differentiation. **j** Quantification of dental pulp cavity percentage in control and mutant mice. $P < 0.0001$. **k** Quantification of distance of *Dspp*⁺ cells to cervical loop in control and mutant mice. $P = 0.0003$. For **e**, **f**, **j** and **k** $n = 3$, each data point represents one animal, with unpaired Student's t-test performed. All data are expressed as the mean \pm SD. Source data are provided as a Source Data file. ** $P < 0.01$, **** $P < 0.0001$. Each experiment was repeated independently three times. White dotted line outlines cervical loop. Cre-: *Rosa-DTA*; Cre+: *Advillin^{CreER};Rosa-DTA*. Scale bars, **g** 1mm; others, 100 μ m.



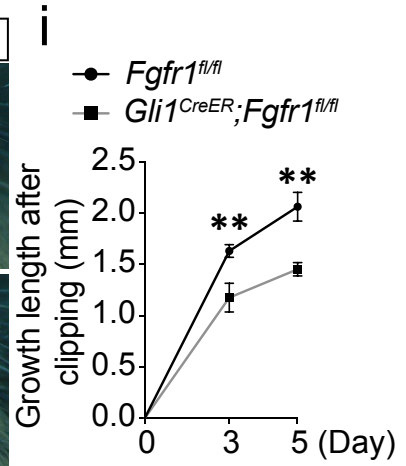
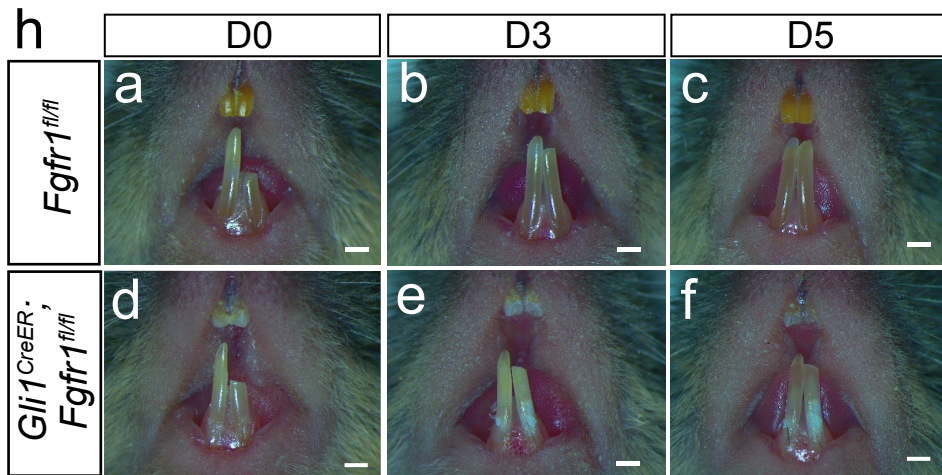
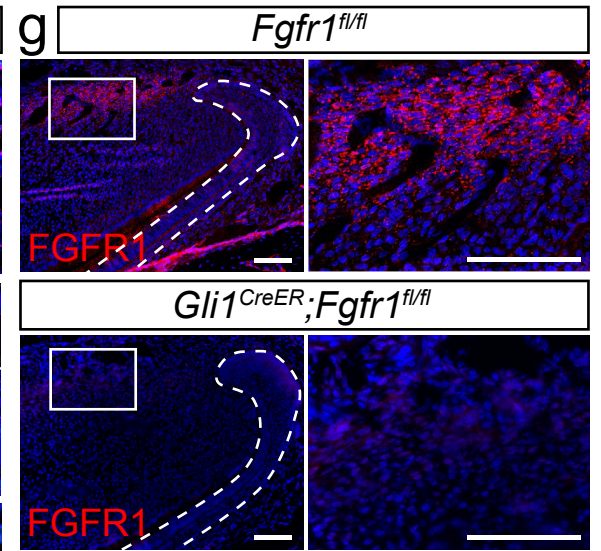
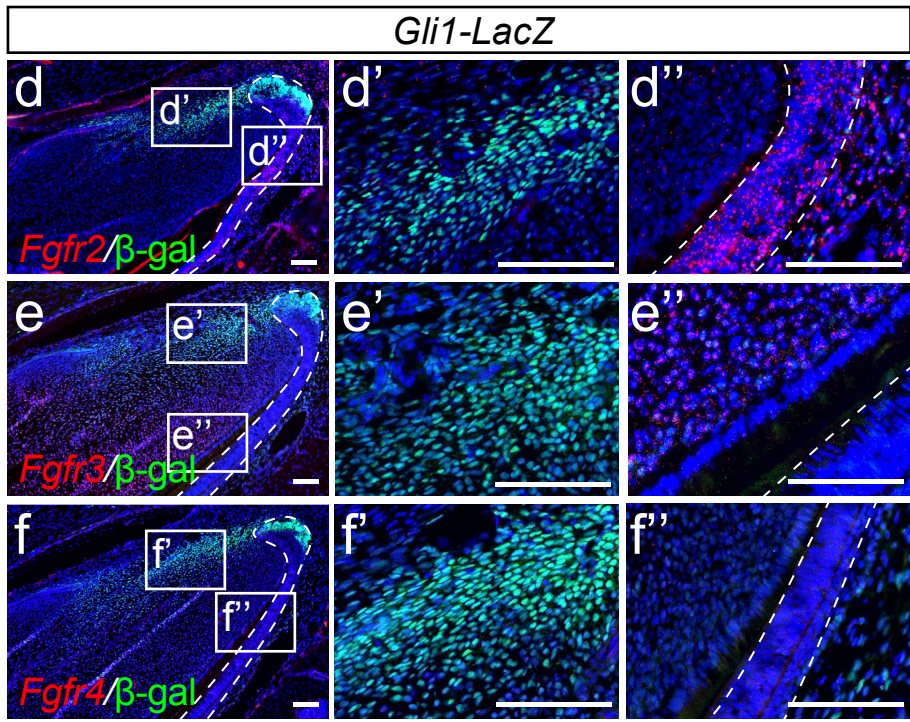
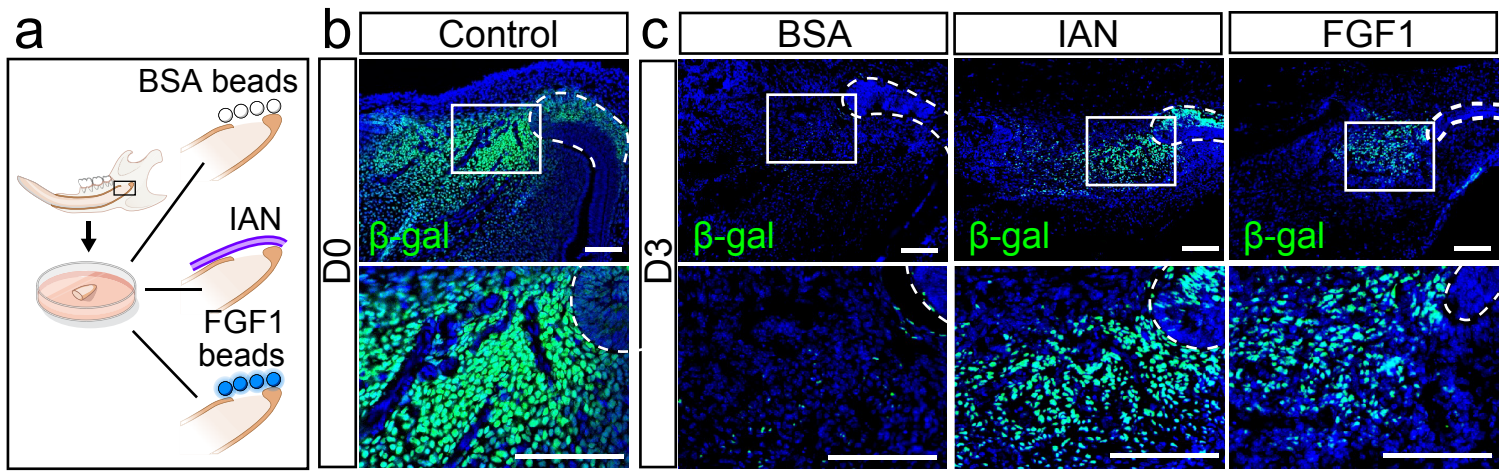
Supplementary Fig. 2: FGF1 is an important ligand secreted from sensory neurons.

a Significant signaling pathways involved in the interaction between the trigeminal ganglion and incisor of an adult mouse. SNI-IV, sensory neuron type I-IV; GC, glia cell; PMC, proximal mesenchymal cell (MSC region); MC, meningeal cell; MS, myelinating Schwann cell; nMS, non-myelinating Schwann cell; MA, macrophage; RBC, red blood cell; DF, dental follicle cell; TAC, TA cell; TC, T cell; OD, odontoblast; MI, microglia; NE, neutrophil; LY, lymphocyte; EC, endothelial cell; GC-DP, glia cell in dental pulp; CC, cycling cell. **b** Schematic illustrating the retrograde fluorescent tracing. **c-d** Fluorescent cells in the trigeminal ganglion. CTB-488⁺ neurons were exclusively detected in the V3 branch of the trigeminal nerve. V1, V2 and V3 indicate the three branches of the trigeminal nerve. White arrowheads point to CTB-488⁺ neurons. **e-l** Mechanosensation neurons innervating incisor secrete FGF1. **e and i** Colocalization of CTB-488, *Gfra2* and *Fgf1* in V3 of trigeminal ganglion. **f and j** CTB-488⁺ neurons in trigeminal ganglion. **g and k** Expression of *Gfra2* in trigeminal ganglion. **h and l** Expression of *Fgf1* in trigeminal ganglion. Yellow arrows indicate CTB-488⁺/*Gfra2*⁺/*Fgf1*⁺ neurons; yellow arrowheads indicate CTB-488⁺/*Fgf1*⁺ neurons. Scale bars, **c**, 500µm; others, 100µm.



Supplementary Fig. 3: FGF ligands in adult mouse incisor.

a-b Feature plot of FGF ligands in adult mouse incisor. **c-d** RNAscope staining of *Fgf3* in the incisor. **e-f** RNAscope staining of *Fgf8* in the incisor. **g-h** Expression of *Fgf9* in the incisor. **i-j** Expression of *Fgf10* in the incisor. White dotted line outlines cervical loop. Scale bars, 100 μ m.



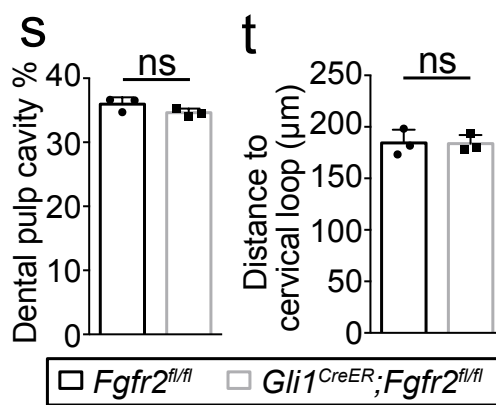
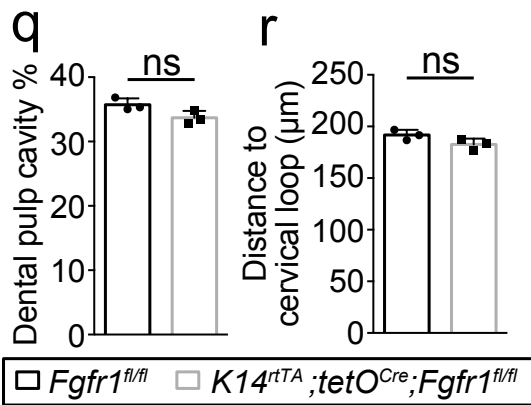
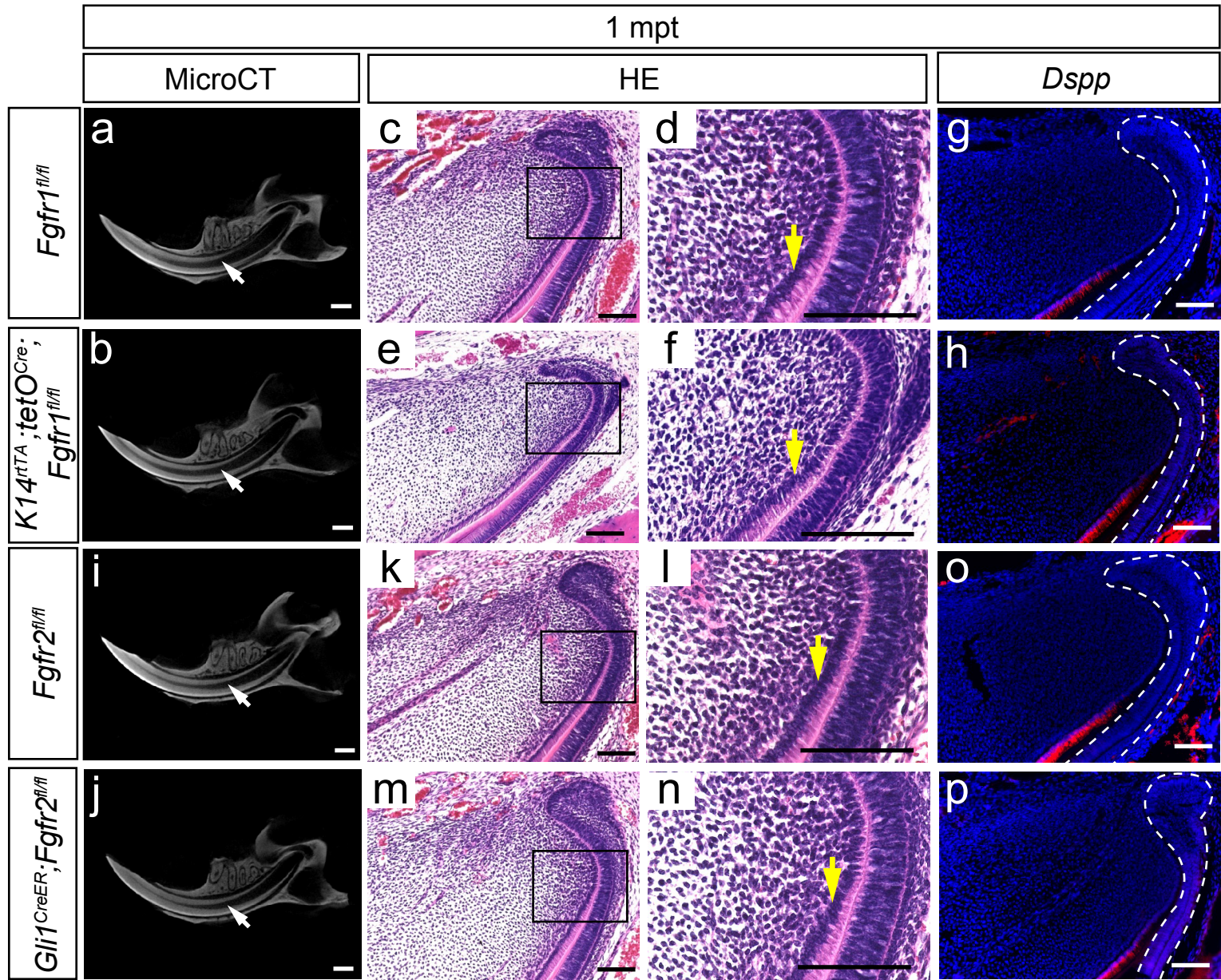
Supplementary Fig. 4: FGF1 secreted from sensory nerves directly acts on MSCs via FGFR1.

a-c FGF1 is crucial for MSC maintenance. **a** Schematic of the incisor explant culture. The proximal ends of *Gli1-LacZ* mouse incisors were cultured with BSA beads, IAN and recombinant FGF1 beads respectively. **b** Expression of *Gli1*⁺ cells in the proximal end of the incisor. **c** *Gli1*⁺ cells labeled with β-gal in incisor explant with BSA beads, IAN surrounding the proximal end or recombinant FGF1 beads cultured for 3 days respectively.

d-f Expression of FGFRs in the incisor. **d** Expression patterns of *Fgfr2* and β-gal in the incisors of *Gli1-LacZ* mice. **e** *Fgfr3* is expressed in the sub-odontoblast layer and in partial pulp cells, but is barely detectable in the proximal end of the incisor. **f** *Fgfr4* expression is undetectable in the incisor.

g FGFR1 was deleted in *Gli1^{CreER};Fgfr1^{fl/fl}* mice. The expression of FGFR1 is shown in control and *Gli1^{CreER};Fgfr1^{fl/fl}* mice.

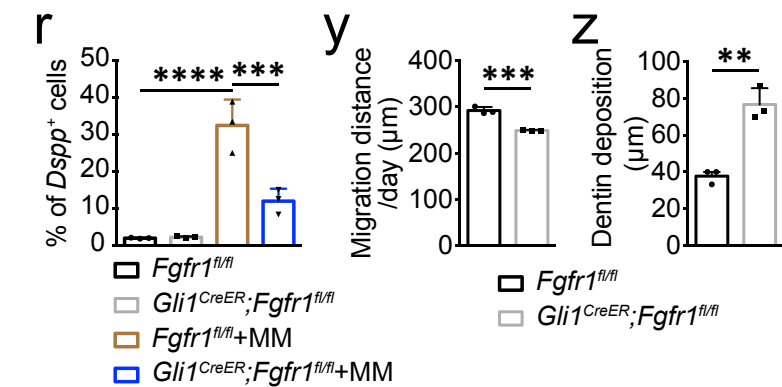
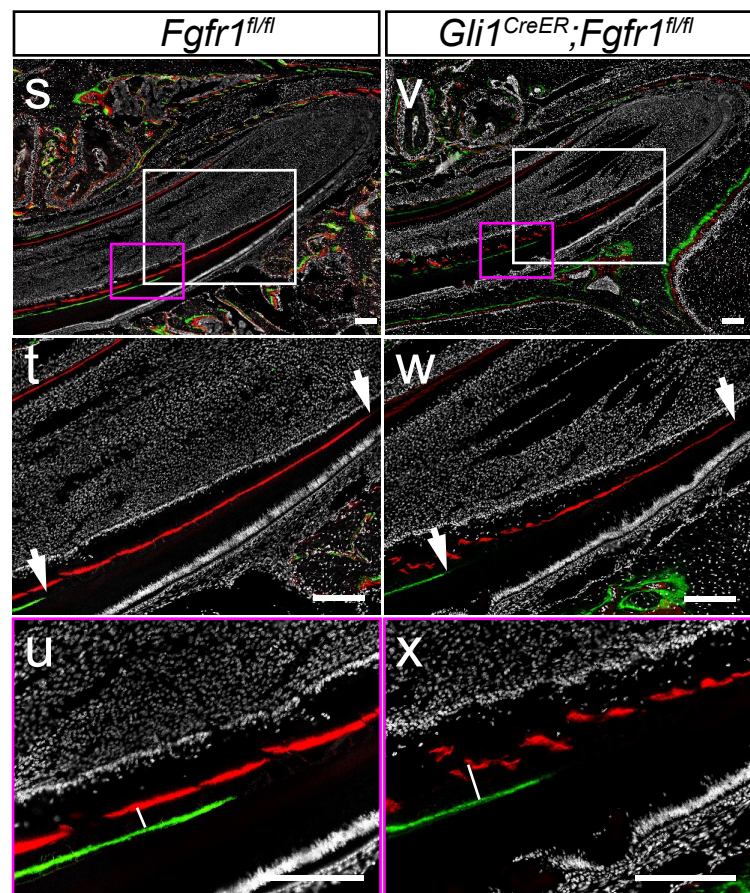
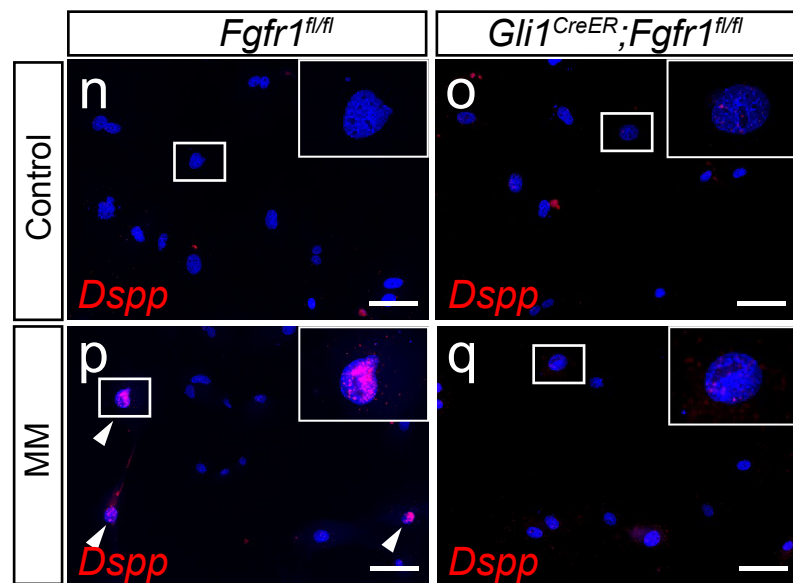
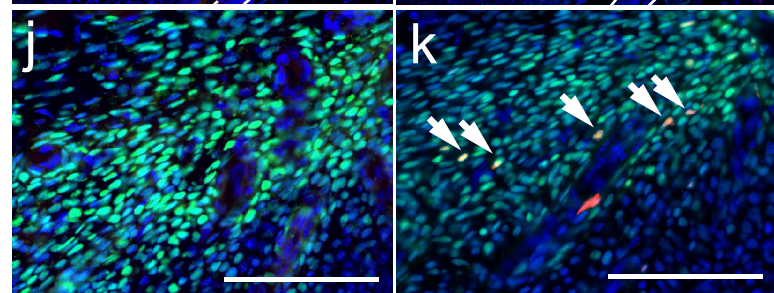
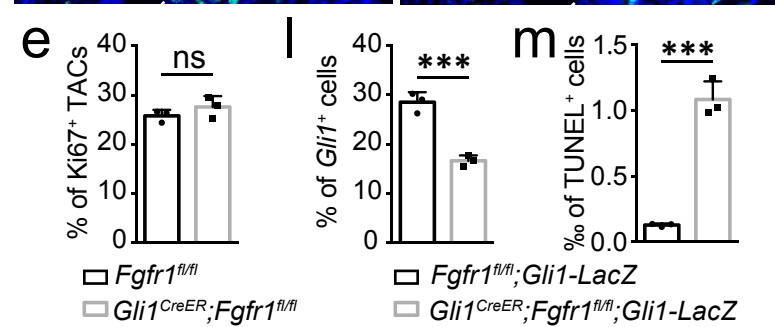
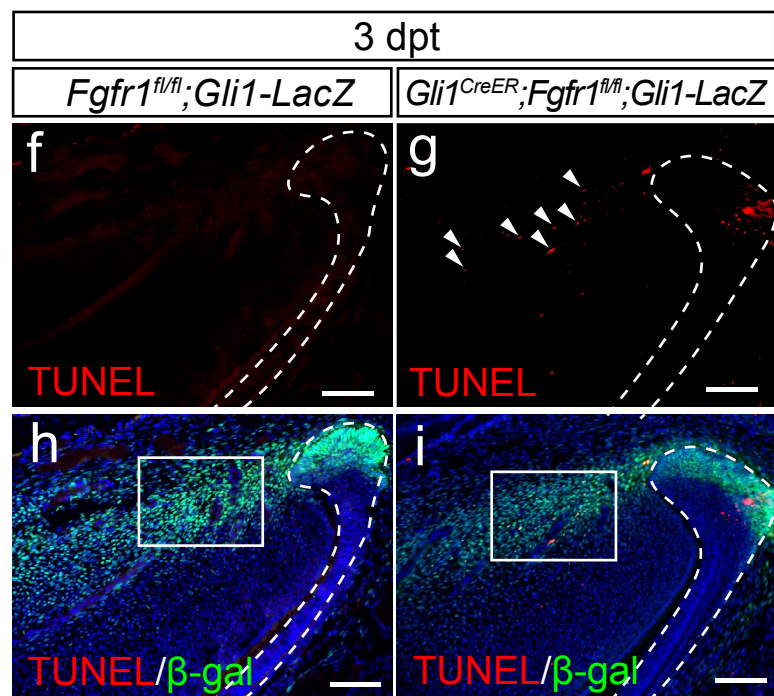
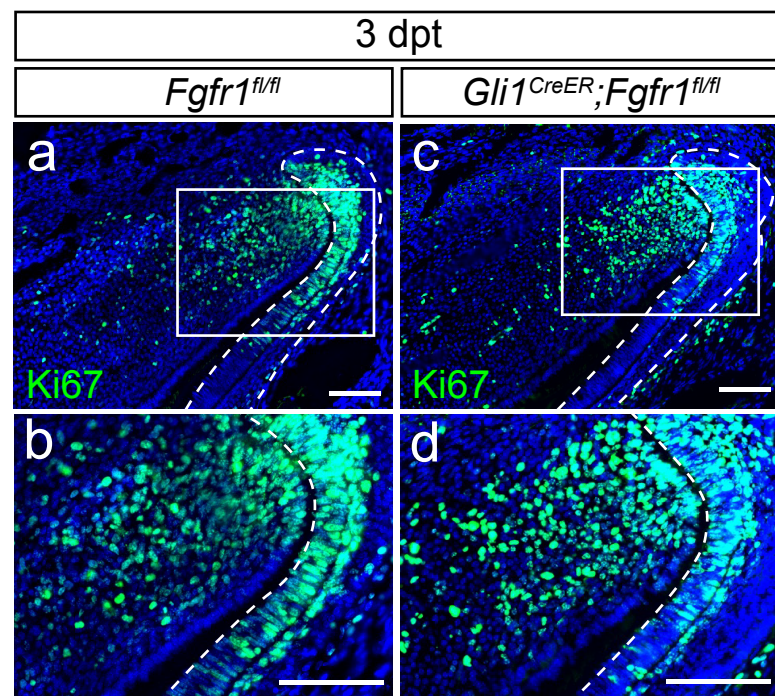
h Tissue repair is impaired after FGF signaling is deleted in MSCs. The incisor was clipped and the subsequent injury repair was observed in control and *Gli1^{CreER};Fgfr1^{fl/fl}* mice on D3 and D5 after clipping. The amount of incisor growth in control and *Gli1^{CreER};Fgfr1^{fl/fl}* mice was analyzed on D3 and D5 after clipping. D3: P=0.0069; D5: P=0.0024. N=3, each data point represents one animal, with unpaired Student's t-test performed. All data are expressed as the mean±SD. Source data are provided as a Source Data file. **P<0.01, ****P<0.0001. Each experiment was repeated independently three times. White dotted line shows the cervical loop. Scale bars, **h** 1mm; others, 100μm.



Supplementary Fig. 5: Neither depletion of FGFR1 in epithelium nor depletion of FGFR2 in MSCs affect mesenchymal homeostasis.

a-h No obvious change in dentin formation is observed when FGFR1 is depleted from the epithelium. **a-b** CT images of control and *K14^{rtTA};tetO^{Cre};Fgfr1^{fl/fl}* mice one month after induction. The morphology with histological analysis (**c-f**) and differentiation of odontoblasts (**g-h**) showed no obvious differences between groups. **q** Quantification of dental pulp cavity percentage in control and mutant mice. P=0.0712. **r** Quantification of distance of *Dspp*⁺ cells to cervical loop in control and mutant mice. P=0.1044.

i-p No obvious change in dentin formation is observed when FGFR2 is depleted in MSCs. **i-j** CT images of control and *Gli1^{CreER};Fgfr2^{fl/fl}* mice one month after induction. The odontoblast morphology (**k-n**) and differentiation (**o-p**) are unaffected in *Gli1^{CreER};Fgfr2^{fl/fl}* mice. **s** Quantification of dental pulp cavity percentage in control and mutant mice. P=0.1428. **t** Quantification of distance of *Dspp*⁺ cells to cervical loop in control and mutant mice. P=0.9412. White arrow points to dental pulp cavity; yellow arrow points to pre-odontoblast. For **q-t** n=3 and each data point represents one animal, with unpaired Student's t-test performed. All data are expressed as the mean±SD. Source data are provided as a Source Data file. **P<0.01, ****P<0.0001. Each experiment was repeated independently three times. White dotted line outlines cervical loop. Scale bars, **a-b** and **i-j** 1mm; others, 100µm.



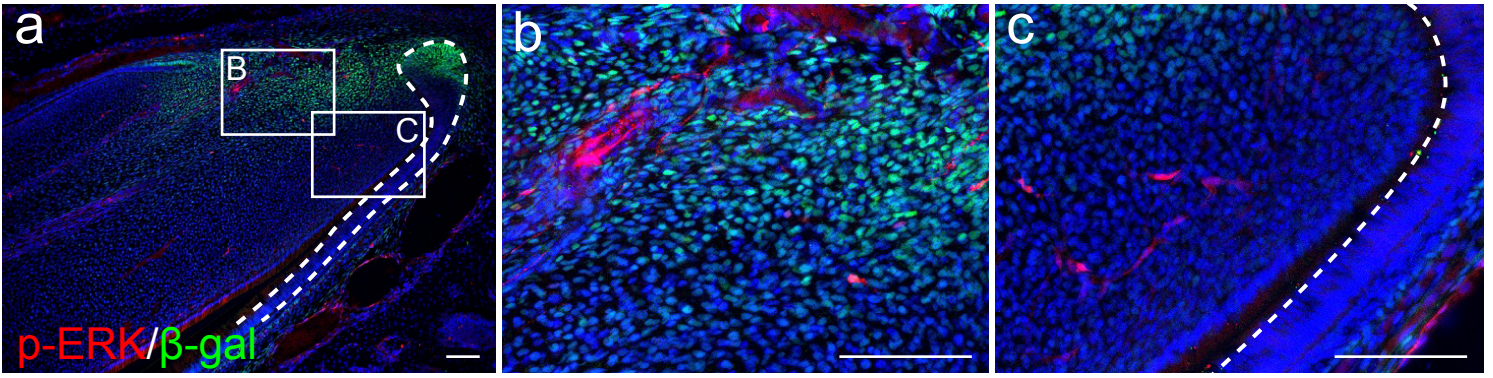
Supplementary Fig. 6: Loss of FGF signaling in MSCs disturbs mesenchymal tissue homeostasis.

a-k Apoptosis leads to decreased MSCs. **a-d** TACs stained with Ki67 in control and *Gli1^{CreER};Fgfr1^{fl/fl}* mice 3 days after induction. **e** Quantification of Ki67⁺ TACs in control and mutant mice. P=0.2817. **f-m** Increased apoptosis in *Gli1*⁺ cells in *Gli1^{CreER};Fgfr1^{fl/fl};Gli1-LacZ* mice. **f-g** Apoptosis detected with TUNEL staining in control and *Gli1^{CreER};Fgfr1^{fl/fl};Gli1-LacZ* mice. White arrowheads point to TUNEL⁺ cells. **h-k** TUNEL and β -gal staining in control and mutant mice. White arrows point to co-localization of TUNEL⁺ cells and *Gli1*⁺ cells. **l** Quantification of *Gli1*⁺ cells in the mesenchyme. P=0.0009. **m** Quantification of TUNEL⁺ cells in the mesenchyme. P=0.0003. N=3, each data point represents one animal, with unpaired Student's t-test performed.

n-r Decreased odontoblastic differentiation of MSCs with FGF signaling depletion. Expression of *Dspp* in cells from control and *Gli1^{CreER};Fgfr1^{fl/fl}* mice, after culturing for 3 days with medium (**n-o**) or mineralized medium (MM) (**p-q**). White arrowhead points to *Dspp*⁺ cells. **r** Quantification of Ki67⁺ TACs in control and mutant mice. *Fgfr1^{fl/fl}* versus *Gli1^{CreER};Fgfr1^{fl/fl}*: P<0.0001; *Fgfr1^{fl/fl}*+MM versus *Gli1^{CreER};Fgfr1^{fl/fl}*+MM: P=0.0009. N=3 each data point represents one biological replicate, with one-way ANOVA analysis.

s-z Decreased migration of odontoblasts with FGF signaling depletion. **s and v** With double labeling by calcein and Alizarin red injection, we can observe the dynamics of dentin formation. **t and w** The length between red and green fluorescence indicates migration of odontoblasts within 5 days. **u and x** The thickness between red and green fluorescence shows the deposition of dentin. White arrows point to the length of odontoblast migration; white lines indicate the thickness of dentin. **y** Quantification of migration distance per day. P=0.0007. **z and e** Quantification of dentin deposition. P=0.0022. N=3, each data point represents one animal, with unpaired Student's t-test performed. All data are expressed as the mean \pm SD. Source data are provided as a Source Data file. **P<0.01, ****P<0.0001. Each experiment was repeated independently three times. White dotted line shows the cervical loop. Scale bars, **s and v** 200 μ m; others, 100 μ m.

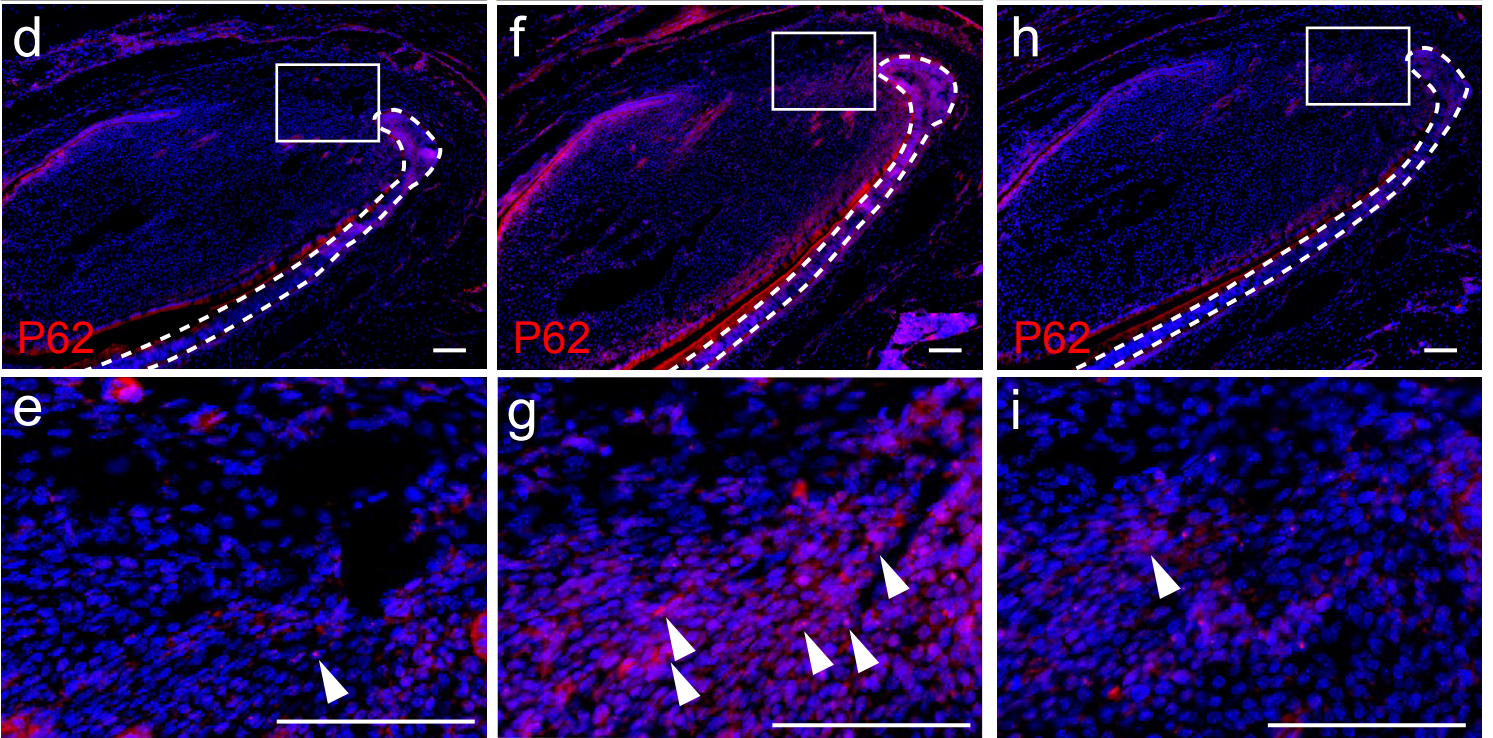
Gli1-LacZ



Fgfr1^{fl/fl}

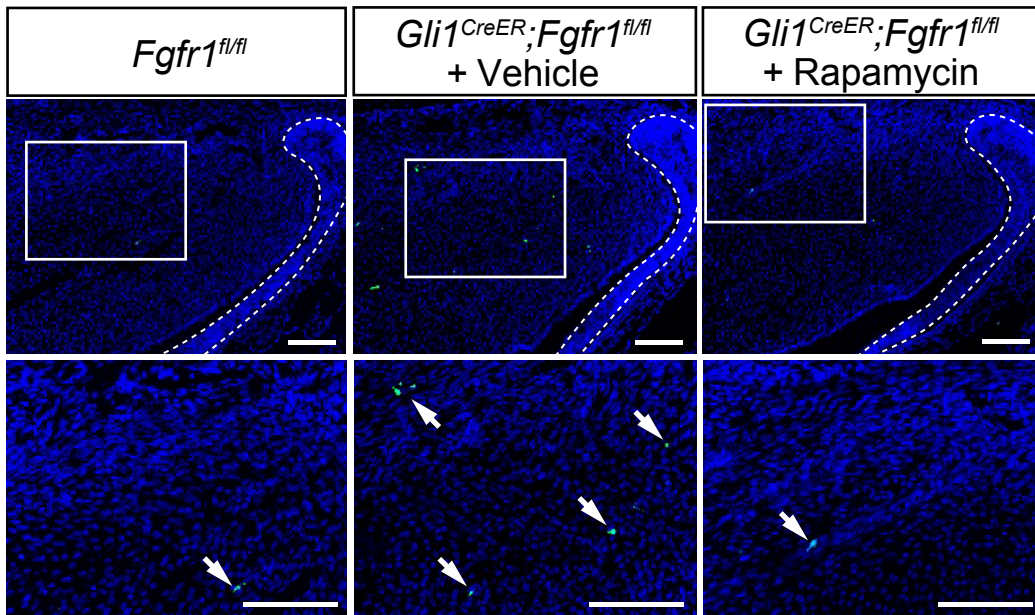
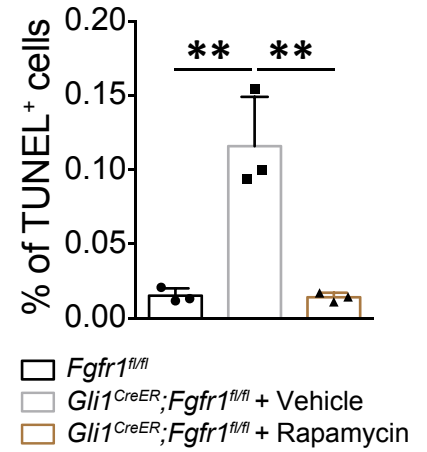
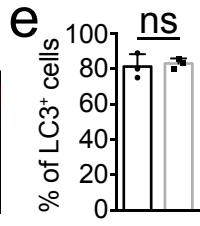
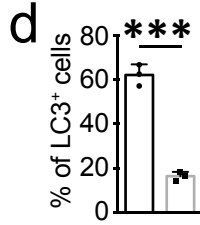
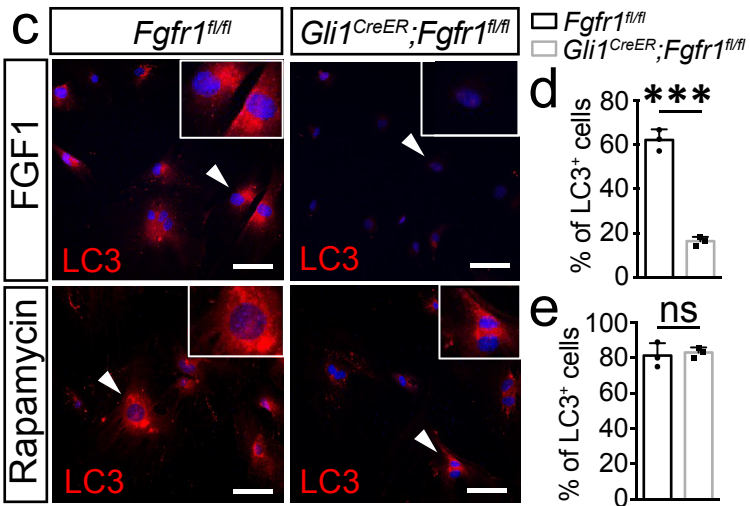
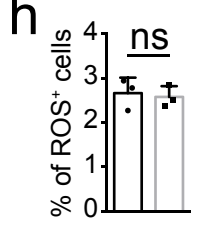
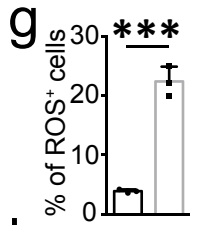
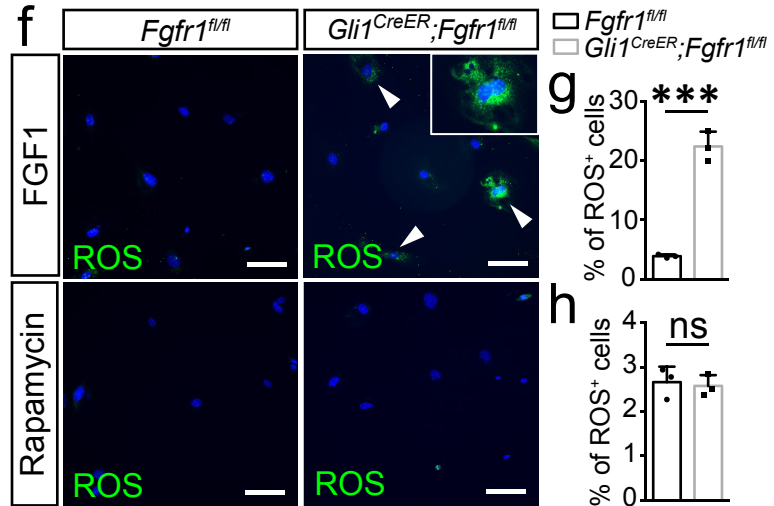
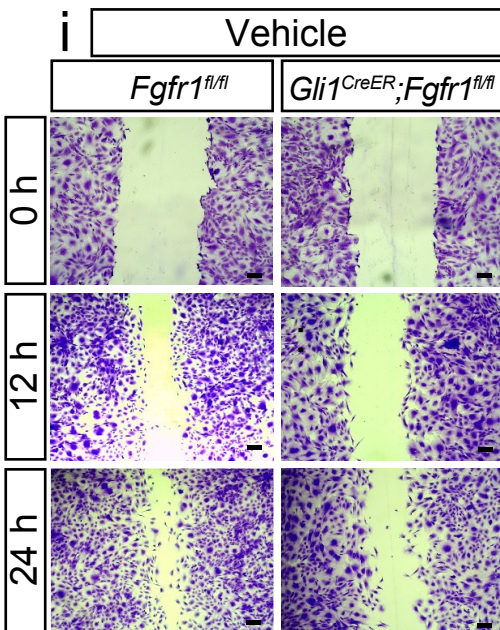
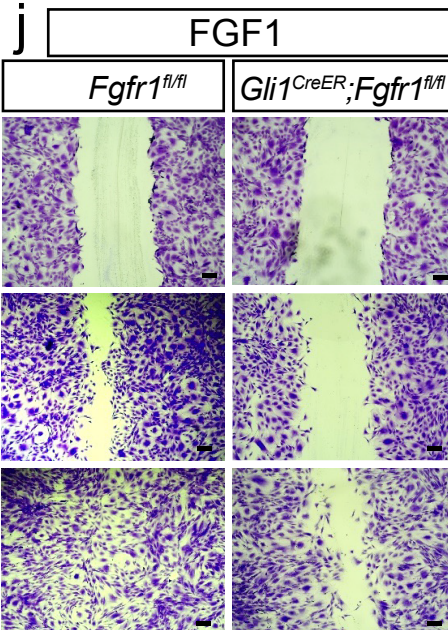
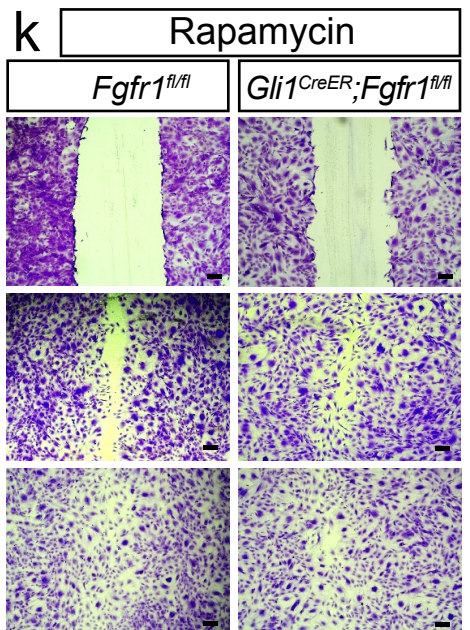
Gli1^{CreER};Fgfr1^{fl/fl}+Vehicle

Gli1^{CreER};Fgfr1^{fl/fl}+Rapamycin



Supplementary Fig. S7: Autophagy is reactivated in *Gli1^{CreER};Fgfr1^{fl/fl}* mice by rapamycin injection.

a-c Expression pattern of p-ERK and β -gal in the incisor of *Gli1-LacZ* mice. **d-i** Expression of autophagy substrate P62 in incisors of control, *Gli1^{CreER};Fgfr1^{fl/fl}* mice treated with vehicle and *Gli1^{CreER};Fgfr1^{fl/fl}* mice treated with rapamycin. White arrowhead points to P62⁺ cells. Scale bars, 100 μ m.

a**b****c****f****i****j****k**

Supplementary Fig. 8: Activation of autophagy provides resistance to apoptosis and promotes cell migration.

a TUNEL⁺ cells in incisors of control, *Gli1^{CreER};Fgfr1^{fl/fl}* mice treated with vehicle and *Gli1^{CreER};Fgfr1^{fl/fl}* mice treated with rapamycin 3 days after tamoxifen induction. White arrows point to TUNEL⁺ cells. **b** Quantification of TUNEL⁺ cells in the mesenchyme. Control versus *Gli1^{CreER};Fgfr1^{fl/fl}* + Veh: P=0.0018; *Gli1^{CreER};Fgfr1^{fl/fl}* + Veh vs *Gli1^{CreER};Fgfr1^{fl/fl}* + Rap: P=0.0017. N=3, each data point represents one animal, with one-way ANOVA analysis. **c** Expression of LC3 in MSCs from control and *Gli1^{CreER};Fgfr1^{fl/fl}* mice with FGF1 or rapamycin treatment. White arrowheads point to cells in inset. **d** Quantification of LC3⁺ cells in control and mutant cells with FGF1 treatment. P=0.0001. **e** Quantification of LC3⁺ cells in control and mutant cells with Rapamycin treatment. P=0.7155. **f** Expression of ROS in MSCs from control and *Gli1^{CreER};Fgfr1^{fl/fl}* mice with FGF1 or rapamycin treatment. White arrowheads point to ROS⁺ cells. **g** Quantification of ROS⁺ cells in control and mutant cells with FGF1 treatment. P=0.0002. **h** Quantification of ROS⁺ cells in control and mutant cells with Rapamycin treatment. P=0.7427. **i-k** Migration of cells from control and *Gli1^{CreER};Fgfr1^{fl/fl}* mice treated with vehicle, FGF1 or rapamycin for 0h, 12h and 24h. For **d**, **e**, **g** and **h**, n=3, each data point represents one biological replicate, with unpaired Student's t-test performed. All data are expressed as the mean±SD. Source data are provided as a Source Data file. **P<0.01, ****P<0.0001. Each experiment was repeated independently three times. White dotted line shows the cervical loop. Scale bars, 100µm.